

RESEARCH

Regulation of epinephrine biosynthesis in *HRAS*-mutant paragangliomas

Minghao Li^{1,2}, Susan Richter³, Hermine Mohr⁴, Stephan Drukewitz^{5,6}, Isabel Poser³, Daniela Stanke³, Bruna Calsina⁷, Angel M Martinez-Montes⁷, Marcus Quinkler⁸, Henri J L M Timmers⁹, Svenja Nölting^{10,11}, Felix Beuschlein^{10,11}, Hanna Remde¹², Giuseppe Opocher¹³, Elena Rapizzi¹⁴, Karel Pacak¹⁵, Christina Pamporaki¹, Mercedes Robledo¹⁶, Longfei Liu¹⁷, Jingjing Jiang¹⁶, Stefan R Bornstein¹, Graeme Eisenhofer¹, Stephanie M J Fliedner¹⁷ and Nicole Bechmann¹⁷

¹Department of Medicine III, University Hospital Carl Gustav Carus, Technische Universität Dresden, Fetscherstrasse, Dresden, Germany

²Department of Urology, Xiangya Hospital, Central South University, Changsha, China

³Institute for Clinical Chemistry and Laboratory Medicine, University Hospital Carl Gustav Carus, Medical Faculty Carl Gustav Carus, Technische Universität Dresden, Dresden, Germany

⁴Institute for Diabetes and Cancer, Helmholtz Centre Munich, Neuherberg, Germany

⁵Institute of Human Genetics, University of Leipzig Medical Center, Leipzig, Germany

⁶Core Unit for Molecular Tumor Diagnostics (CMTD), National Center for Tumor Diseases (NCT), Partner Site Dresden, Dresden, Germany

⁷Hereditary Endocrine Cancer Group, Spanish National Cancer Research Center and Centro de Investigación Biomédica en Red de Enfermedades Raras (CIBERER), Madrid, Spain

⁸Endocrinology in Charlottenburg, Berlin, Germany

⁹Department of Internal Medicine, Radboud University Medical Center, Nijmegen, The Netherlands

¹⁰Medizinische Klinik Und Poliklinik IV, Klinikum der Ludwig-Maximilians-Universität München, Munich, Germany

¹¹Department of Endocrinology, Diabetology and Clinical Nutrition, Universitätsspital Zürich (USZ) and University of Zurich (UZH), Zurich, Switzerland

¹²Division of Endocrinology and Diabetes, Department of Internal Medicine I, University Hospital of Würzburg, Würzburg, Germany

¹³Department of Medicine, University of Padua, Padua, Italy

¹⁴Department of Experimental and Clinical Medicine, University of Florence, Italy

¹⁵Section on Medical Neuroendocrinology, Eunice Kennedy Shriver National Institute of Child Health and Human Development, National Institutes of Health, Bethesda, Maryland, United States

¹⁶Department of Endocrinology and Metabolism, Zhongshan Hospital, Fudan University, Shanghai, China

¹⁷University Cancer Center Schleswig-Holstein, University Medical Center Schleswig-Holstein, Lübeck, Germany

Correspondence should be addressed to N Bechmann: Nicole.bechmann@uniklinikum-dresden.de

Abstract

The biochemical phenotype of paragangliomas (PGLs) is highly dependent on the underlying genetic background and tumor location. PGLs at extra-adrenal locations usually do not express phenylethanolamine *N*-methyltransferase (PNMT), the enzyme required for epinephrine production, which was explained by the absence of glucocorticoids. PGLs with pathogenic variants (PVs) in Harvey rat sarcoma viral oncogene homolog (*HRAS*) can occur in or outside of the adrenal, but always synthesize epinephrine independently of the localization. Here, we characterize the signaling pathways through which PVs in *HRAS* influence *PNMT* expression. Catecholamines, cortisol, and transcriptional features of PGL tissues with known genetic background were analyzed. Genetically modified rat pheochromocytoma cells carrying PVs in *Hras* were generated and analyzed for regulation of *Pnmt* expression. Elevated epinephrine contents in PGLs with PVs in *HRAS* were accompanied by enrichment in mitogen-activated protein kinase (MAPK) signaling compared to PGLs with PVs in genes that activate hypoxia pathways. *In vitro*, *Hras* PVs increased *Pnmt* expression and epinephrine biosynthesis through increased phosphorylation of stimulatory protein 1 via MAPK signaling. Here, we provide a molecular mechanism that explains the PV-dependent epinephrine production of PGLs.

Keywords

- ▶ paraganglioma
- ▶ catecholamines
- ▶ glucocorticoids
- ▶ MAPK pathway
- ▶ phenotype-genotype correlations

Endocrine-Related Cancer
(2023) 30, e230230

Introduction

Paragangliomas (PGLs) are neuroendocrine tumors that originate from neural crest-derived cells of the sympathetic and parasympathetic ganglia. PGLs that arise from chromaffin cells of the adrenal medulla are named pheochromocytomas (PCCs) (Mete *et al.* 2022). Most PCCs and PGLs (together PPGLs) are characterized by the biosynthesis, storage, and secretion of catecholamines (dopamine, norepinephrine, and epinephrine). Although rare, PPGL can be lethal as excessive catecholamine secretion can result in life-threatening cardiovascular complications (Lenders *et al.* 2020).

The biosynthesis of catecholamines starts with the uptake of L-tyrosine by chromaffin cells, which is subsequently converted by a series of enzymes to L-3,4-dihydroxyphenylalanine, dopamine, and norepinephrine (Fig. 1A). Finally, the enzyme phenylethanolamine N-methyltransferase (PNMT) catalyzes the conversion from norepinephrine to epinephrine. In addition to the catecholamine-producing chromaffin cells of the medulla, the adrenal gland contains a second endocrine tissue, the steroid-producing cortex. Glucocorticoids from the adrenal cortex diffuse to chromaffin cells and bind to glucocorticoid receptors (GRs) that subsequently induce transcription of *PNMT* expression (Fig. 1B) (Bohn *et al.* 1984, Berends *et al.* 2019). In addition

to glucocorticoid-dependent induction of *PNMT* expression, transcription factors such as stimulatory protein 1 (SP1), early growth response protein 1 (EGR1), activator protein 2 (AP2), and c-Myc-associated zinc finger protein (MAZ) can bind to the *PNMT* promoter (Fig. 1B) (Huynh *et al.* 2006, Berends *et al.* 2019). According to classical understanding, glucocorticoids of the adrenal cortex prevail in the regulation of epinephrine biosynthesis in the adrenal medulla (Wurtman & Axelrod 1965). Thus, it was assumed that only PCCs derived from adrenal medulla are capable of synthesizing epinephrine while those from extra-adrenal paraganglia are not, due to a lack of glucocorticoid-induced expression of *PNMT* (Eisenhofer *et al.* 2005, 2020).

Recent studies showed a strong genotype-phenotype correlation in PPGLs (Eisenhofer *et al.* 2011, Crona *et al.* 2019). Tumors with pathogenic variants (PVs) in genes that lead to activation of hypoxia signaling pathways (cluster 1), such as genes encoding succinate dehydrogenase subunits A–D (*SDHx*), fumarate hydratase (*FH*), von Hippel-Lindau (*VHL*) tumor suppressor, endothelial PAS domain protein 1 (*EPAS1* or *HIF2α*), prolyl hydroxylase domain-containing proteins 1/2 (*PHD1/2*) and isocitrate dehydrogenase 1/2 (*IDH1/2*), are unable to synthesize epinephrine due to a lack of *PNMT* expression (Fishbein *et al.* 2017). Cluster 1 PPGLs are characterized by an increased expression and stabilization of hypoxia-inducible factor 2α (*HIF2α*),

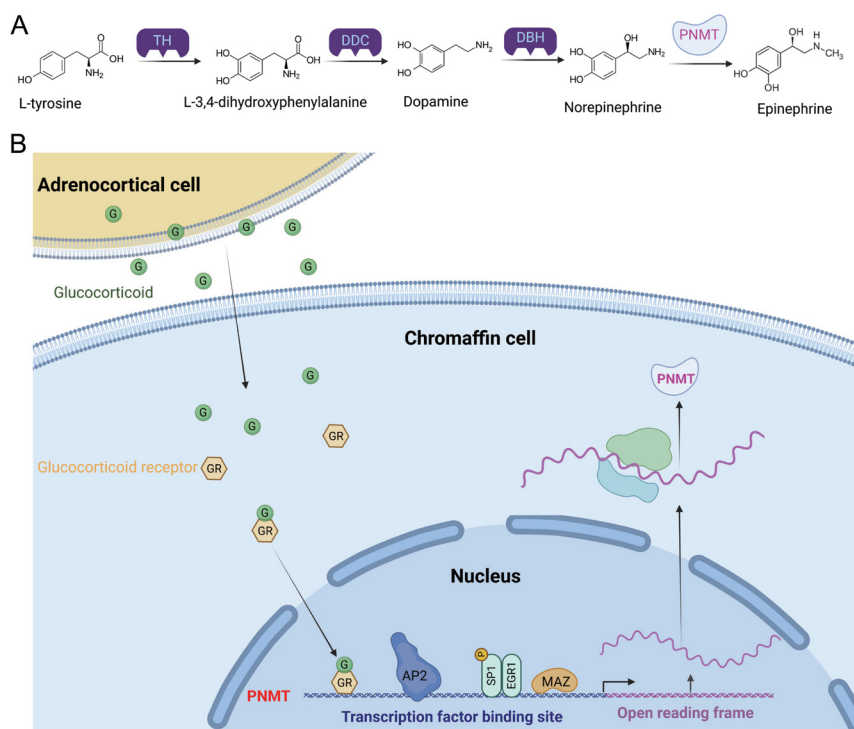


Figure 1

Regulation of catecholamine biosynthesis in chromaffin cells of the adrenal medulla. (A) L-tyrosine is converted into L-3,4-dihydroxyphenylalanine (L-DOPA) by tyrosine hydroxylase (TH), which is subsequently converted into dopamine and norepinephrine by the enzymes, DOPA decarboxylase (DDC) and dopamine beta-hydroxylase (DBH). The enzyme phenylethanolamine N-methyltransferase (PNMT) catalyzes the final conversion from norepinephrine into epinephrine. (B) Several transcription factors, such as glucocorticoid receptor (GR), activator protein 2 (AP2), stimulatory protein 1 (SP1), early growth response protein 1 (EGR1), and c-Myc-associated zinc finger protein (MAZ) regulate the expression of *PNMT* in chromaffin cells of the adrenal medulla. The binding of GR to the *PNMT* promoter requires activation through glucocorticoids (G) that are secreted from the adrenal cortex.

which blocks glucocorticoid-mediated induction of PNMT (Qin *et al.* 2014). In contrast, tumors with PVs in genes that activate kinase signaling (cluster 2), such as RET protooncogene (*RET*), neurofibromin 1 (*NF1*), Harvey rat sarcoma viral oncogene homolog (*HRAS*), MYC-associated factor X (*MAX*), and transmembrane protein 127 (*TMEM127*), are able to synthesize epinephrine and are characterized by a more mature catecholamine secretory machinery compared with cluster 1 PPGLs (Eisenhofer *et al.* 2004, Fishbein *et al.* 2017). While epinephrine-producing cluster 2 PPGLs occur almost exclusively in the adrenal, norepinephrine-producing cluster 1 PPGLs can arise at both adrenal and extra-adrenal locations (Crona *et al.* 2019, Eisenhofer *et al.* 2020). In addition, there is a third cluster comprising PPGLs with activation of the Wnt-signaling pathway.

In a Sino-European study, we identified 29 extra-adrenal PGLs capable of epinephrine biosynthesis, almost all cases were identified in the Chinese population and the majority of them carried somatic PVs in *HRAS* (Jiang *et al.* 2020). This suggests that the underlying PV, rather than tumor location or proximity to the glucocorticoid-secreting adrenal cortex, is responsible for the epinephrine-producing phenotype of PPGLs. However, mechanistic investigations to this end are not available. The present study used PPGL specimens and genetically engineered cell line models to explore the mechanism of how PVs in *HRAS* affect PNMT expression and subsequent epinephrine production.

Materials and methods

All solutions and reagents were of the highest purity available from Sigma Aldrich GmbH unless otherwise stated. Cell culture medium and additives were purchased from Gibco (Thermo Fisher Scientific), except for fetal calf serum (Biowest, Riverside, MO, USA).

Patient cohort and clinical samples

Tumor tissues of patients diagnosed with PPGL were obtained from 11 recruiting centers: University Hospital Carl Gustav Carus Dresden, Germany; University Medical Centre Schleswig-Holstein Lübeck, Germany; University Hospital of Munich, Germany; University Hospital of Würzburg, Germany; Radboud University Medical Centre, Nijmegen, the Netherlands; Endocrinology in Charlottenburg, Berlin, Germany; Spanish National

Cancer Research Center (CNIO), Madrid, Spain; Veneto Institute of Oncology, IRCCS, Padova, Italy; University of Florence, Italy; and National Institutes of Health (NIH), Bethesda, USA. Patients were included in the Prospective Monoamine-producing Tumor study (PMT study) and/or the Registry and Repository of biological samples of the European Network for the Study of Adrenal Tumors (ENS@T) or the NIH with ethics approval at each institution. Informed consent was obtained from all patients. Genetic testing was performed as described earlier (Currás-Freixes *et al.* 2017, Li *et al.* 2023).

Catecholamine measurements

Measurements of tumor tissue catecholamines were performed using liquid chromatography with electrochemical detection as described elsewhere (Eisenhofer *et al.* 1986). PPGL tissues of 251 patients were included in the study and were either lysed using 0.4 M perchloric acid containing 0.5 mM EDTA in Milli-Q water or an aqueous buffer system as described elsewhere (Eisenhofer *et al.* 1986, Bechmann *et al.* 2021).

PNMT enzyme activity and cortisol measurements

PNMT enzyme activity and cortisol levels in PPGL tissues were determined as previously described (Qin *et al.* 2013, Bechmann *et al.* 2021).

Transcriptome data

Transcriptional data from 177 PPGLs was obtained from a published cohort deposited in the European Genome-Phenome Archive (EGA) (EGAS00001006044) and processed as described (Calsina *et al.* 2023). Differential expression analysis was executed between PPGLs with PVs in *HRAS* ($n=33$), cluster 1- ($n=86$) and/or other cluster 2-related PVs ($n=58$) using DESeq2 v1.18.1 (Love *et al.* 2014). Results of the DESeq2 analyses were filtered for significant P -values ($P_{adj} < 0.05$) and visualized using the python seaborn package. The gene set enrichment analysis was done using gseapy package on KEGG pathway database (Kanehisa 2022, Fang *et al.* 2023).

Cell culture

The rat PCC cell line, PC12, was obtained from Interlab Cell Line Collection (https://bioinformatics.hsanmartino.it/iclc/en_indexp.html). Cells were cultured

with RPMI1640 containing 5% fetal bovine serum and 10% horse serum (complete medium) at 37°C, 5% CO₂, and 95% humidity (Bechmann *et al.* 2019). MycoAlert Mycoplasma Detection Kit (Lonza, Basel, Switzerland) was used to confirm that cells were mycoplasma free. After trypsinization (trypsin-EDTA; 0.05%:0.02%), cells were diluted with complete medium and counted using C-CHIPs (Neubauer improved). Cultivation and experiments were performed using collagen-coated cell culture dishes.

Hras PV editing

Two hotspot PVs in *Hras*, G13R and Q61R, were introduced into PC12 cells using CRISPR/Cas9-based prime editing (Anzalone *et al.* 2019). The experimental procedure is described in detail in the supplement. For cell culture experiments, three G13R mutant clones, PC12 *Hras* G13R K4, PC12 *Hras* G13R K6, and PC12 *Hras* G13R K12, and two control clones of G13R, PC12 *Hras* G13R Ctrl1 and Ctrl2, were used (Supplementary Fig. 1, see section on [supplementary materials](#) given at the end of this article). In parallel, two Q61R mutant clones, PC12 *Hras* Q61R K9 and PC12 *Hras* Q61R K11, and two control clones of Q61R, PC12 *Hras* Q61R Ctrl1 and Ctrl2, were investigated (Supplementary Fig. 1). Data from the different clones – mutant or control – of the same PV were presented pooled. The comparison of the individual clones is shown in the supplementary data.

Cell growth assay

A total of 1.5×10^5 cells were seeded in six-well plates. After cultivation for 48, 72, or 144 h, cells were washed with PBS, trypsinized, re-suspended, and counted using C-CHIPs. Each well was counted in duplicate.

Adhesion assay

A total of 2.5×10^5 cells were seeded in six-well plates (pre-culture). After 24 h incubation, cells were seeded to collagen-coated 24-well plates that were blocked with PBS containing 2% BSA for 1 h at 37°C. After 60 min incubation, non-attached cells were removed by washing with PBS. The adherent cells were fixed, stained, and dried on air overnight as previously described (Bechmann *et al.* 2020). The stained cells were dissolved using PBS containing 0.5% Triton-X-100 and absorption was measured at 550 nm (reference 650 nm) by Spark® multimode microplate reader (Tecan Group Ltd., Männedorf, Switzerland).

Migration and invasion assay

The capacity of cells to actively migrate and invade through 8 µm pores was examined using TC-Inserts (Sarstedt AG and Co. KG, Nümbrecht, Germany) as previously described (Bechmann *et al.* 2020).

Catecholamine biosynthesis/storage in PC12 cell lines

Cells (1×10^5) were seeded in 24-well plates. After cell adhesion, cells were treated with dexamethasone (1 µM) or DMSO as control. Cells were incubated for 48 h, washed with PBS, extracted, and analyzed as described earlier.

Trametinib treatment

Cells (1×10^6) were seeded in T25-flasks. After 24 h, cells were treated with trametinib (1 µM; Biomol GmbH, Hamburg, Germany). Samples for RNA and protein isolation were collected 48 h after treatment.

RNA isolation and qRT-PCR

RNA was isolated using NucleoSpin RNA Plus Kit (Macherey-Nagel GmbH, Düren, Germany) in accordance with the manufacturer's instructions. Reverse transcription and qRT-PCR were performed as previously described (Bechmann *et al.* 2020). Primer sequences are listed in Supplementary Table 2.

SDS-PAGE and western blot analysis

Preparation of cell lysates, separation of proteins via SDS-PAGE, western blot transfer, and protein visualization were performed as previously described (Bechmann *et al.* 2018). Antibodies are listed in Supplementary Table 3. Densitometric analyses were performed with ImageJ.

HRAS activity assay

To determine the activity of HRAS in PC12 clones with and without PV in *Hras*, HRAS activity assay (ab211158) was used in accordance with the manufacturer's instructions (details in supplementary data).

Statistical analysis

Experiments were repeated in three or four different cell passages (biological replicates). Descriptive data

were expressed as mean \pm S.E.M. with statistical analyses taking into consideration numbers (n) of biological and technical replicates within independent experiments. Statistical analyses were carried out by *t*-test, Mann-Whitney *U* test, or Kruskal-Wallis test with *post hoc* Bonferroni test using SigmaPlot 12.5 (Systat Software GmbH, Erkrath, Germany).

Results

Molecular characterization of *HRAS*-mutant PPGLs

To investigate the molecular features of PPGLs with PVs in *HRAS*, we examined 251 PPGL specimens with known genetic background (130 cluster 1 PPGLs; 106 cluster 2 PPGLs (*HRAS*-mutant PPGLs excluded), 15 *HRAS*-mutant PPGLs) for their tissue catecholamine content (Fig. 2A). Of the 15 *HRAS*-mutant PPGLs, 2 were extra-adrenal PGLs. Regardless of tumor location, *HRAS*-mutant PPGLs showed comparable tissue epinephrine contents and PNMT enzyme activities to the other cluster 2 PPGLs, while they differed from cluster 1 PPGLs (Fig. 2B). Similarly, the dopamine, norepinephrine, and total catecholamine content of PPGLs showed a similar relation, with decreased levels in cluster 1 PPGLs compared to *HRAS*-mutant and the other cluster 2 PPGLs (Supplementary Fig. 2). Of note, in cluster 1 PPGLs, the extra-adrenal location was associated with reduced contents of norepinephrine and epinephrine compared to tumors located within the adrenal (Fig. 2B and Supplementary Fig. 2). Gene expression profiles were examined to identify molecular differences that may contribute to the phenotypic features of *HRAS*-mutant PPGLs. *HRAS*-mutated PPGLs exhibited high concordance with the other cluster 2 PPGLs at mRNA level (214 upregulated and 193 genes downregulated), whereas 3269 genes were upregulated and 3712 genes were downregulated compared to cluster 1 PPGLs (Fig. 2C). Pathway enrichment analysis revealed that *HRAS*-mutated PPGLs were enriched in pathways of cancer, dopaminergic synapse and mitogen-activated protein kinase (MAPK) signaling pathway, among others, compared to cluster 1 PPGLs (Fig. 2D).

Genome editing of *Hras* PVs in PC12 cells and their influence on cellular phenotype

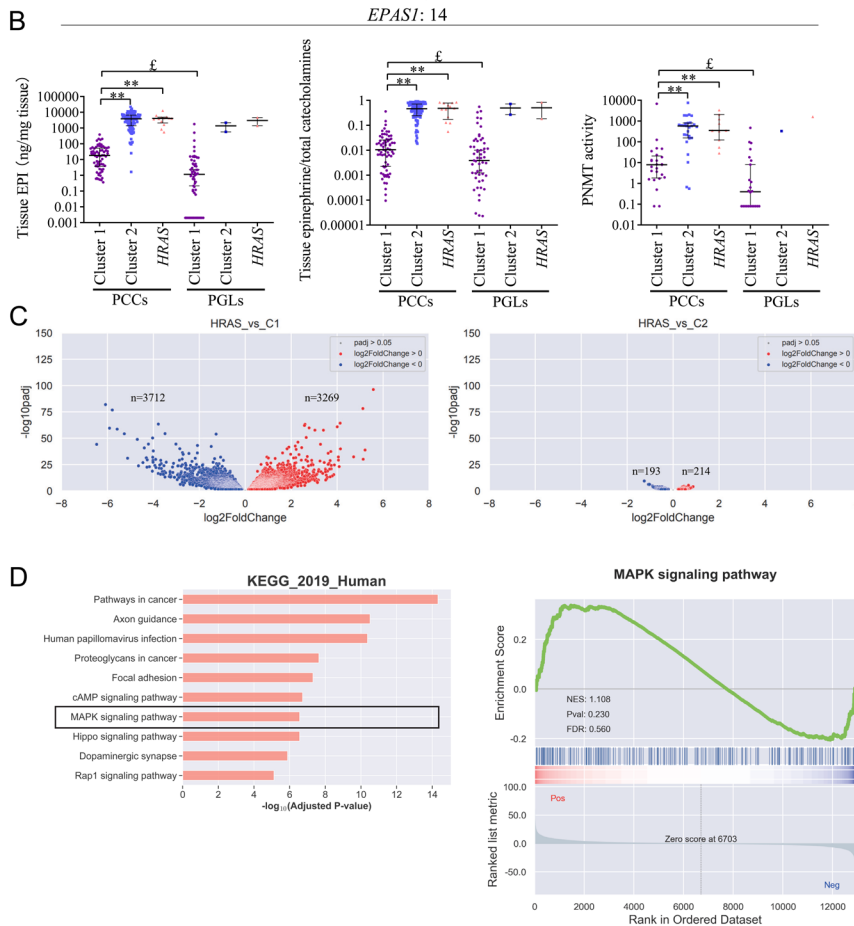
To understand the molecular mechanisms of our previous findings (Fig. 2 and (Jiang *et al.* 2020)), we generated a *Hras*-dependent cell line model that mimics

the *HRAS* tumor phenotype *in vitro*. Therefore, we introduced two well-known gain-of-function hotspot PVs of *HRAS* -G13R and Q61R (Stenman *et al.* 2016)- into PC12 cells using CRISPR/Cas9-based prime editing. Both PVs have been previously reported in PPGLs (Crona *et al.* 2013, Jiang *et al.* 2020) and in our cohort (Fig. 2A). Sanger sequencing verified the success of genetic editing in three or two different clones per gene variant (Supplementary Fig. 1). To confirm the functionality of the obtained PC12 *Hras*-mutant clones, we tested for the active, guanosine triphosphate bound form of HRAS. Introduction of *Hras* PVs increased the level of active HRAS compared to control cells (Fig. 3A and Supplementary Fig. 3A), whereas total levels of HRAS were not affected (Fig. 3B and Supplementary Fig. 3B). The RAS family of oncoproteins includes two other members, KRAS and NRAS, with a similar function. To determine whether the introduced PVs in *Hras* also affected these oncoproteins, we examined protein expression. NRAS was reduced by the introduction of *Hras* PVs in PC12 cells, while KRAS remained unaffected (Fig. 3B and Supplementary Fig. 3B). *Hras*-mutant cells exhibited a lower growth rate than control clones (Fig. 3C and Supplementary Fig. 4A). Compared to control clones, *Hras*-mutant clones showed a higher adhesion ability to collagen (Fig. 3D and Supplementary Fig. 4B), lower migration, and invasion capacity (Fig. 3E, F, Supplementary Fig. 4C and D).

PVs in *Hras* upregulate *Pnmt* expression and induce epinephrine biosynthesis in PC12 cells

Next, we characterized epinephrine biosynthesis in relation to HRAS activation. Compared to the control clones, *Hras*-mutant clones showed significantly higher *Pnmt* expression (G13R mutants: 16.8–38.8-fold; Q61R mutants: 3.5–4.8-fold; Fig. 4A and Supplementary Fig. 5A). Epinephrine was measurable in all three PC12 clones with *Hras* G13R PV, while it was undetectable in the control clones and *Hras* Q61R mutant clones (Fig. 4B and Supplementary Fig. 6A). *Th* expression was also increased in *Hras*-mutant clones, while no clear trend was observed for *Ddc* and *Dbh* expression when PC12 *Hras*-mutant clones were compared to control clones (Supplementary Fig. 7). In addition, clones with *Hras* PVs showed higher levels of phosphorylated TH S40 (Supplementary Fig. 8A and B), a well-known phosphorylation site associated with an increased TH enzyme activity (Dunkley *et al.* 2004). Clones with

A	Cluster 1	Cluster 2	<i>HRAS</i>
Patient	130	106	15
Sex (female: male)	61:69	56:40 [§]	8:7
Age, medians (IQR) (year)	34.0 (22.0-46.0)	45.2 (36.0-54.0)	51.7 (40.8-58.0)
Location			
- Adrenal	68	104	13
- Extra-adrenal	57	2 [¶]	2
- Adrenal + extra-adrenal	5	0	0
Tumor size, medians (IQR) (cm)	2.7 (1.8-3.8)	3.9 (2.6-5.6)	3.9 (3.4-5.0)
Metastasis [#]	19.1% (18/94)	3.6% (3/83)	13.3% (2/15)
Pathogenic variant	<i>VHL</i> : 57 <i>SDHA</i> : 2 <i>SDHB</i> : 34 <i>SDHC</i> : 3 <i>SDHD</i> : 16 <i>FH</i> : 3 <i>MDH2</i> : 1 <i>EPAS1</i> : 14	<i>RET</i> : 59 <i>NF1</i> : 38 <i>TMEM127</i> : 4 <i>MAX</i> : 5	<i>HRAS</i> G13R: 3 <i>HRAS</i> Q61R: 4 <i>HRAS</i> Q61K: 3 <i>HRAS</i> Q61A: 3 NA: 2



Hras PV displayed a higher dopamine content than control clones (Supplementary Fig. 9A and B), which is consistent with elevated dopamine and total catecholamine contents in PPGL tissues with PVs in *HRAS* compared to cluster 1 PPGLs (Supplementary Fig. 2A and C).

Hras PVs upregulate *Pnmt* expression through phosphorylation of SP1 via MAPK pathway

Since the MAPK pathway is one of the ten most regulated pathways in *HRAS*-mutated PPGLs compared to cluster 1

PPGLs (Fig. 2D), we further investigated this pathway in our *Hras*-dependent cell line model to gain insight into its modulatory effect on *Pnmt* expression. *Hras*-mutant clones showed a significantly higher expression of pERK1/2 T202/Y204 than control clones (Fig. 4C and Supplementary Fig. 10), which confirms activation of the MAPK signaling pathway in *Hras*-mutant clones. Inhibition of the MAPK pathway with the MEK inhibitor, trametinib, resulted in a significant reduction of pERK1/2 level in all clones, leading to a decrease in *Pnmt* expression in the *Hras*-mutant clones, while control clones were unaffected (Fig. 4D, E, F, Supplementary

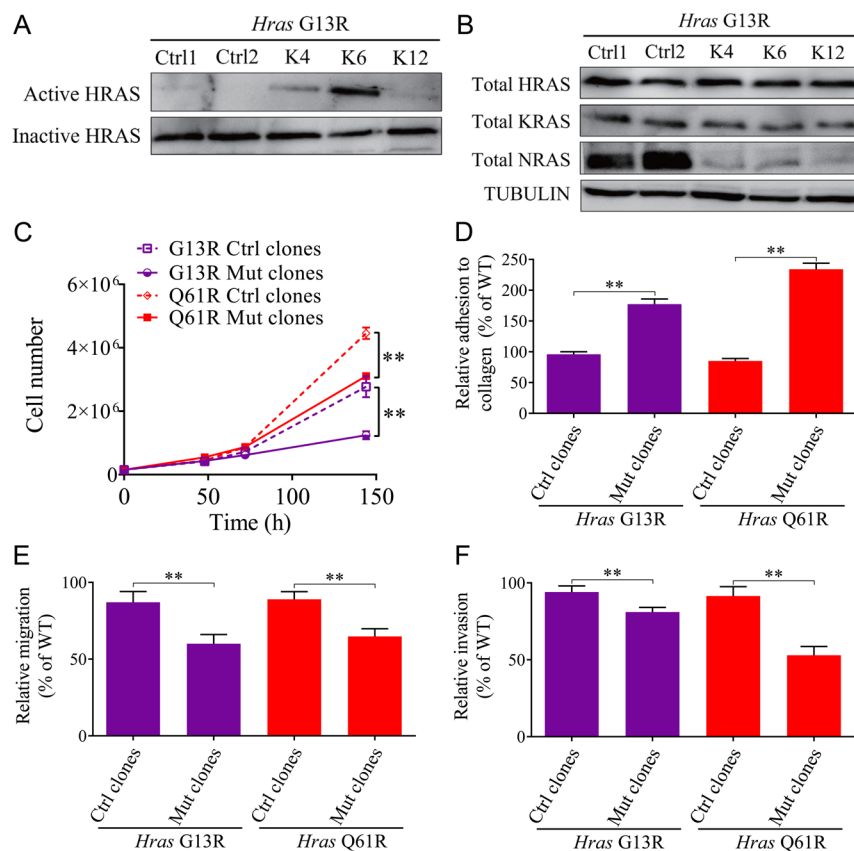


Figure 3

Cell characteristics of PC12 cells with or without pathogenic variants (PVs) in *Hras*. (A) PC12 clones with *Hras* G13R PV (PC12 *Hras* G13R K4, K6, K12) showed elevated levels of active HRAS compared to control clones (PC12 *Hras* G13R Ctrl1, Ctrl2), while inactive HRAS remained comparable. (B) Total expression of HRAS and KRAS did not differ between *Hras* G13R mutant and control clones, while NRAS expression was diminished in PC12 *Hras* G13R mutant clones compared to control clones. Shown are representative sections of four independent experiments. (C) *Hras* mutant (Mut) PC12 clones showed a diminished growth rate compared to control clones. (D) Clones with *Hras* PV exhibited an increased adhesion ability to collagen than control clones. Clones with *Hras* PV showed a lower migration (E) and invasion (F) capacity than respective control clones. Comparisons between control clones and *Hras*-mutant clones were carried out by *t*-test, **P* < 0.05, ***P* < 0.01. Four independent experiments were performed (*n* = 12). Data of the individual *Hras*-mutant and control clones are shown in the supplementary data (Supplementary Fig. 4).

Fig. 10 and 11). SP1 is phosphorylated by the MAPK pathway (Malumbres & Barbacid 2003), which is essential for the transport of SP1 into the nucleus and respective binding to the *PNMT* promoter binding site (Her *et al.* 2003). In our cell model, pSP1 was mainly located in the nucleus, while SP1 was found in the cytoplasm rather than in the nucleus (Supplementary Fig. 12A and B). Treatment with trametinib decreased pSP1 levels in both *Hras*-mutant and control clones, while SP1 levels increased along with the reduction of pERK1/2 (Fig. 4D, E, F and Supplementary Fig. 10).

PVs in *Hras* mediate glucocorticoid sensitivity in PC12 cells

PCCs present with significantly higher tumor cortisol contents than PGLs (Fig. 5A). While tumor location had no effect on epinephrine, norepinephrine, and total catecholamine contents of cluster 2 PPGLs, intra-adrenal cluster 1 PPGLs presented with significantly higher epinephrine, norepinephrine, and total catecholamine contents than extra-adrenal cluster 1 PPGLs (Fig. 2B). Although the number of cluster 2 extra-adrenal PPGLs is limited, this suggests that the biosynthesis/storage of epinephrine in cluster 2 PPGLs, including

HRAS-mutated PPGLs, may be largely independent of access to glucocorticoids. To investigate this further, we treated our cell line models with the glucocorticoid dexamethasone, which is known to induce *PNMT* in PC12 cells (Byrd *et al.* 1986). Dexamethasone treatment led to increased expression of *Pnmt* in control clones, while no effect was observed in *Hras*-mutant clones (Fig. 5B and Supplementary Fig. 5B). Dexamethasone treatment also failed to increase the epinephrine contents in *Hras* G13R mutant clones (Fig. 5C), which might indicate reduced sensitivity to glucocorticoids in *HRAS*-mutant PPGLs. Overall, epinephrine levels in all clones were very low or even below the detection limit.

We then investigated GR expression in our *Hras*-dependent cell line models to gain further insight into the reduced sensitivity of *HRAS*-mutant PPGLs to glucocorticoids. GR levels were significantly diminished in *Hras*-mutant clones compared to control clones, while *Nr3c1* (encoding for GR) expression was overall comparable or slightly increased in *Hras*-mutant clones (Fig. 5D, E, Supplementary Fig. 13 and 14). Next, we analyzed GR protein in PPGL tissues and identified comparable levels in cluster 1, *HRAS*-mutant and cluster 2 PPGLs, while *HRAS*-mutant PPGLs showed the highest levels of *PNMT* compared to cluster 1 and 2 PPGLs (Fig. 5F).

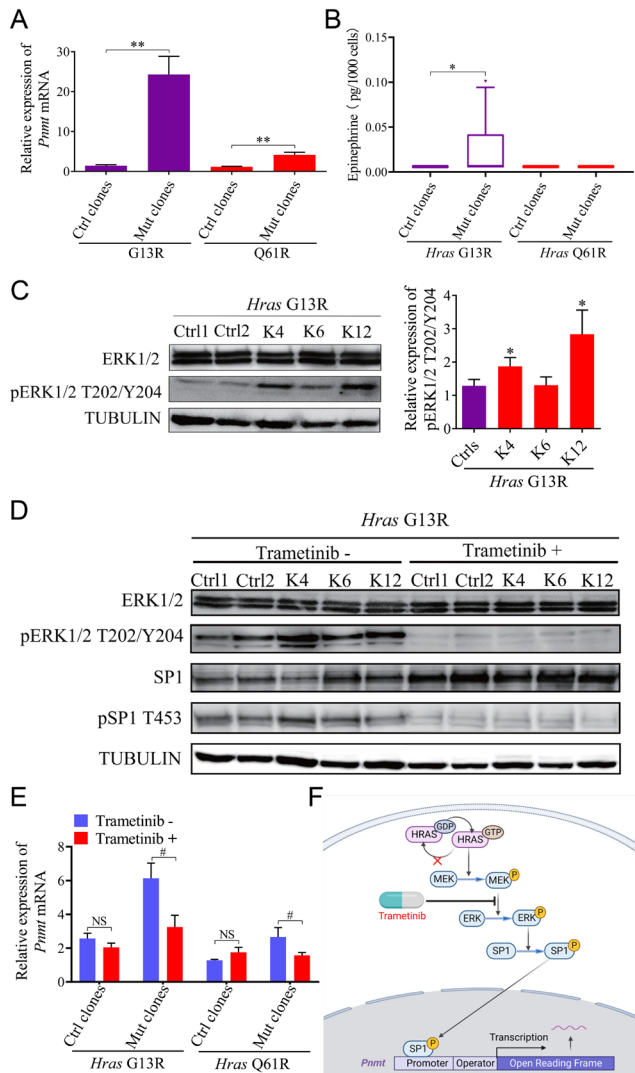


Figure 4
 Pathogenic variants (PVs) in *Hras* upregulate *Pnmt* expression and epinephrine biosynthesis via activation of MAPK signaling in PC12 cells. (A) PC12 clones with PV in *Hras* exhibited higher *Pnmt* expression than control clones. (B) Epinephrine was undetectable in PC12 control clones, PVs in *Hras* G13R, but not in Q61R, resulted in detectable levels of epinephrine in the PC12 cells. (C) PC12 clones with *Hras* G13R PV showed higher levels of phosphorylated ERK than control clones, which indicates a stronger activation of MAPK signaling pathway in *Hras* G13R mutant than control clones. (D) Treatment with the MEK inhibitor, trametinib (1 μ M), decreased the levels of phosphorylated ERK and phosphorylated SP1, while total SP1 expression increased in both *Hras* G13R mutant and control clones. Comparable results were obtained for Q61R mutant clones (Supplementary Fig. 5, 6, and 10). (E) Treatment with trametinib resulted in a significant downregulation of *Pnmt* expression in *Hras*-mutant clones, while control clones were unaffected. (F) Postulated mechanism: *Hras* gain-of-function PVs lead to enhanced phosphorylation of SP1 through the induction of the MAPK signaling pathway. The phosphorylated SP1 subsequently migrates into the nucleus and binds to *Pnmt* transcription factor binding site, thereby transcriptionally stimulating the expression of *Pnmt*. In line with this, inhibition of MAPK pathway by trametinib treatment reduced the level of phosphorylated SP1 and *Pnmt* expression in *Hras*-mutant cells. Created with <https://www.biorender.com/>. For western blot analysis, representative sections of four

Discussion

The findings of our observational study support previous conclusions that PVs are primarily responsible for different catecholamine phenotype of tumors rather than the proximity of chromaffin tumor cells to adrenal glucocorticoids (Jiang *et al.* 2020). Here, we have identified a mechanism of how PVs in *HRAS* modulate epinephrine biosynthesis, which explains the occurrence of epinephrine-producing extra-adrenal PGLs with PVs in *HRAS*. *In vitro*, PVs in *Hras* lead to upregulation of *Pnmt* through MAPK signaling-mediated phosphorylation of SP1. Meanwhile, *Hras*-mutant cells showed decreased sensitivity to glucocorticoid action (Fig. 6).

Germline or somatic PVs can be identified in about 70% of PPGL, and a pronounced correlation between genotype and clinical phenotype appears to exist (Fig. 6) (Crona *et al.* 2019). Nevertheless, it was assumed that cluster 2 PPGLs, which occur predominantly in the adrenal, have an epinephrine-producing phenotype due to their close proximity to glucocorticoids from the adrenal cortex, whereas cluster 1 PPGLs do not express *PNMT* due to their extra-adrenal localization and increased expression and stabilization of HIF2 α (Bechmann & Eisenhofer 2022). HIF2 α represses the transcription of *PNMT* and contributes to a pro-metastatic phenotype of PPGLs (Qin *et al.* 2014, Bechmann *et al.* 2020). Here, we confirmed that PCCs have higher levels of cortisol than PGLs; however, cluster 1 PGLs can contain considerable amounts of cortisol (Supplementary Fig. 15) but fail to produce epinephrine in similar concentrations. Previous findings also demonstrated that catecholamine biosynthesis is not only driven by the close environment in which the tumor develops, thus suggesting that glucocorticoids alone are not sufficient to regulate catecholamine biosynthesis in PPGLs (Grouzmann *et al.* 2015). Besides GR, SP1, and HIF2 α , other factors including AP2, MAZ, and EGR1 can regulate *PNMT* transcription. A study comparing PPGLs with PVs in *VHL* and *RET* showed no differences in *MAZ*, *GR*, and *EGR1* expression (Huynh *et al.* 2006).

We observed a negative regulation of GR levels and a reduced sensitivity to glucocorticoid-mediated induction of *Pnmt* in *Hras*-mutant cells. Attenuation of GR by

independent experiments were shown. For all other experiments, four independent experiments were performed ($n = 12$). Comparisons between control clones and *Hras*-mutant clones were carried out using *t*-test, * $P < 0.05$, ** $P < 0.01$. Comparisons between the same clone treated with and without trametinib were carried out using *t*-test, # $P < 0.05$. Data of the individual *Hras*-mutant and control clones are shown in the supplementary data (Supplementary Fig. 11).

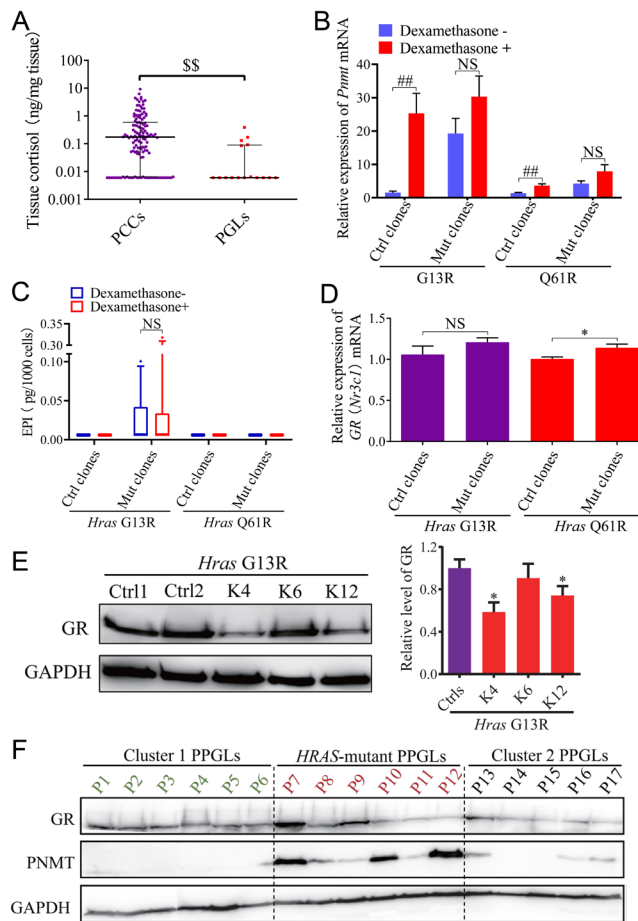


Figure 5
 Glucocorticoid-independent regulation of *PNMT* expression and epinephrine biosynthesis in PPGLs due to pathogenic variants (PVs) in *HRAS*. (A) Tissue cortisol levels were elevated in adrenal PCCs ($n = 47$) compared to extra-adrenal PGLs ($n = 13$). Mann-Whitney *U* test, $^{**}P < 0.01$. (B) Treatment with dexamethasone significantly increased *Pnmt* expression in control clones, but only slightly in *Hras*-mutant clones. Four independent experiments were performed ($n = 12$). Comparisons between same clones treated with or without dexamethasone were carried out using *t*-test, $^{\#}P < 0.05$. (C) Treatment with dexamethasone did not alter the detectable epinephrine (EPI) contents in the *Hras*-dependent PC12 cells. Four independent experiments were performed ($n = 12$). NS: not significant. (D) Expression of *GR* mRNA was in trend increased in *Hras*-mutant compared to control clones. Four independent experiments were performed ($n = 12$). Comparisons between control clones and clones with *Hras* PV were carried out using *t*-test, $^*P < 0.05$. (E) GR levels were significantly reduced in PC12 clones with *Hras* G13R PV compared to control clones. Representative sections of four independent western blot analysis. Data of the individual *Hras*-mutant and control clones are shown in the supplementary data (Supplementary Fig. 5B, 6B, 13 and 14). (F) Glucocorticoid receptor was expressed in all PPGLs, while *PNMT* expression was not detectable in PPGLs due to PVs in cluster 1 genes (P1-2: *SDHA*; P3: *SDHC*; P4-5: *VHL*; P6: *EPAS1*) and some PPGLs due to PVs in cluster 2 genes (P13-15: *NF1*; P16-17: *RET*).

HRAS activation was also described in mouse fibroblasts (Martins *et al.* 1995), and activation of MAPK signaling is discussed as a common mechanism of glucocorticoid resistance, which supports our findings (Sevilla *et al.* 2021). On the other hand, unoccupied GR inhibits *KRAS* signaling and downstream pro-tumorigenic events, whereas glucocorticoids abolish such effects (Caratti *et al.* 2022). Glucocorticoids have also the ability to induce the glucocorticoid-induced leucine zipper that blocks the RAS/RAF phosphorylation cascade (Ayroldi *et al.* 2002). Additionally, it needs to be considered that GR action depends on several posttranslational modifications and cofactors that could further modify the tumor phenotype (Vandevyver *et al.* 2014).

In addition to PVs in *HRAS*, somatic PVs in *FGFR1* and one case of *NF1* mutated PPGL were associated with the occurrence of extra-adrenal PGLs that exhibit an epinephrine-producing phenotype (Jiang *et al.* 2020). These cases were also almost exclusively patients of Chinese origin, which suggests differences in the development of these tumors between the European and Chinese populations. Importantly, gain-of-function PVs in *FGFR1* lead to downstream activation of the RAS-MAPK pathway (Welander *et al.* 2018) and might follow a similar mechanism as PPGLs with PVs in *HRAS*. Unfortunately, information on the biochemical phenotype of these PPGL cases is not available.

Transcriptional profiles of *HRAS*-mutant PPGLs revealed strong overlap with transcriptional profiles of cluster 2 PPGLs, while the differences between *HRAS*-mutant and cluster 1 PPGLs were significant and more distinct. This confirms the previous assignment of *HRAS*-mutant PPGLs to expression cluster 2 (Stenman *et al.* 2016, Fishbein *et al.* 2017). Besides MAPK signaling, RAS activation through PVs in *NF1*, *FGFR1*, or *HRAS* leads to initiation of phosphoinositide 3-kinase, Ral guanine nucleotide dissociation stimulator, and phospholipase C-epsilon signaling (Lim & Leprivier 2019); however, how these pathways influence transcription of *PNMT* remains unknown. Whether the activation of another RAS family member (Lim & Leprivier 2019) has different effects on *PNMT* transcription also remains unclear. In our model, *HRAS* activation led to decreased *NRAS* levels, while *KRAS* remained unchanged.

The increased phosphorylation of SP1 and the modulation of GR levels in *HRAS*-mutant PPGLs does not only modulate *PNMT* expression. Activation of *HRAS* decreased the growth rate and pro-metastatic

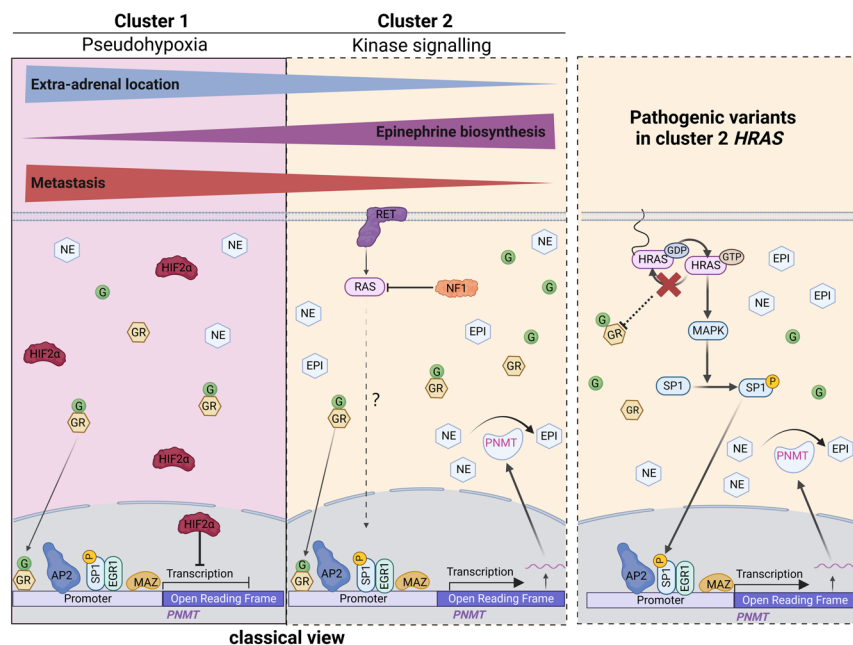


Figure 6

Postulated mechanism for the regulation of PNMT expression in PPGLs with pathogenic variants (PVs) in *HRAS* compared to cluster 1 PPGLs and other cluster 2 PPGLs. In pseudohypoxic cluster 1 PPGLs where PVs in TCA cycle-related genes or genes regulating hypoxia signaling are affected, phenylethanolamine *N*-methyltransferase (*PNMT*) transcription is blocked by increased stabilization of hypoxia-inducible factor 2 α (HIF2 α). Cluster 1 PPGLs occur at adrenal or extra-adrenal locations and are characterized by a norepinephrine-producing phenotype and higher disease aggressiveness. Cluster 2 PPGLs occur almost exclusively in the adrenal gland, where access to glucocorticoids from the adrenal cortex induces *PNMT* expression. Cluster 2 PPGLs which carry PVs that lead to the activation of kinase signaling pathways are therefore characterized by an epinephrine-producing phenotype and have a lower propensity to metastasize than cluster 1 PPGLs. PVs in *HRAS* are assigned to cluster 2 PPGLs; however, they can also occur extra-adrenally. Here, we postulate a mechanism of how PVs in *HRAS* modulate *PNMT* expression. PVs in *HRAS* cause activation of HRAS, which leads to enhanced phosphorylation of SP1 through the induction of the mitogen-activated protein kinase (MAPK) signaling pathway. The phosphorylated SP1 subsequently migrates into the nucleus and binds to the *PNMT* transcription factor binding site, thereby transcriptionally stimulating the expression of *PNMT*. EPI, epinephrine; G, glucocorticoid; NE, norepinephrine. Created with <https://www.biorender.com/>.

features of our cells, suggesting a higher degree of differentiation, which is consistent with increased *Pnmt* expression. The more differentiated phenotype of cluster 2 PPGLs is also accompanied by a less aggressive behavior compared to cluster 1 PPGLs (Bechmann *et al.* 2020). PC12 cells lack expression of the PPGL susceptibility gene *Max*. PPGLs due to PVs in *MAX* fall within the transcription cluster 2 but exhibit an intermediate catecholamine phenotype between clusters 1 and 2 (Qin *et al.* 2014). Therefore, it might be conceivable that *HRAS* activation in PC12 cells shifts the biochemical phenotype toward more differentiated cluster 2 traits.

In conclusion, we identified a mechanism by which PVs in *HRAS* modulate epinephrine biosynthesis via activation of MAPK signaling and downstream phosphorylation of SP1.

Supplementary materials

This is linked to the online version of the paper at <https://doi.org/10.1530/ERC-23-0230>.

Declaration of interest

The authors declare that they have no conflict of interest.

Funding

This study was supported by the Deutsche Forschungsgemeinschaft (DFG, German Research Foundation) within the CRC/Transregio 205/1, Project No. 314061271 - TRR205 'The Adrenal: Central Relay in Health and Disease' and by the Immuno-TargET project under the umbrella of University Medicine Zurich. M.R. was supported by PI20/01169 (Istituto de Salud Carlos III (ISCIII), Acci3n Estrat3gica en Salud, cofinanciado a trav3s del Fondo Europeo de Desarrollo Regional (FEDER)) and Paradifference Foundation (no grant number applicable to M.R.). L.L. was supported by the National Natural Science Foundation of China (No. 82170806). M.L. was funded by China Scholarship Council (No. 201906370033).

References

Anzalone AV, Randolph PB, Davis JR, Sousa AA, Koblan LW, Levy JM, Chen PJ, Wilson C, Newby GA, Raguram A, *et al.* 2019 Search-and-replace genome editing without double-strand breaks or donor DNA. *Nature* **576** 149–157. (<https://doi.org/10.1038/s41586-019-1711-4>)
 Ayroldi E, Zollo O, Macchiarulo A, Di Marco B, Marchetti C & Riccardi C 2002 Glucocorticoid-induced leucine zipper inhibits the Raf-

- extracellular signal-regulated kinase pathway by binding to Raf-1. *Molecular and Cellular Biology* **22** 7929–7941. (<https://doi.org/10.1128/MCB.22.22.7929-7941.2002>)
- Bechmann N, Ehrlich H, Eisenhofer G, Ehrlich A, Meschke S, Ziegler CG & Bornstein SR 2018 Anti-tumorigenic and anti-metastatic activity of the sponge-derived marine drugs Aeropylinin-1 and Isofistularin-3 against pheochromocytoma in vitro. *Marine Drugs* **16** 172. (<https://doi.org/10.3390/md16050172>)
- Bechmann N, Poser I, Seifert V, Greunke C, Ullrich M, Qin N, Walch A, Peitzsch M, Robledo M, Pacak K, *et al.* 2019 Impact of extrinsic and intrinsic hypoxia on catecholamine biosynthesis in absence or presence of HIF2 α in pheochromocytoma cells. *Cancers* **11** 594. (<https://doi.org/10.3390/cancers11050594>)
- Bechmann N, Moskopp ML, Ullrich M, Calsina B, Wallace PW, Richter S, Friedemann M, Langton K, Flidner SMJ, Timmers HJLM, *et al.* 2020 HIF2 α supports pro-metastatic behavior in pheochromocytomas/paragangliomas. *Endocrine-Related Cancer* **27** 625–640. (<https://doi.org/10.1530/ERC-20-0205>)
- Bechmann N, Watts D, Steenblock C, Wallace PW, Schürmann A, Bornstein SR, Wielockx B, Eisenhofer G & Peitzsch M 2021 Adrenal hormone interactions and metabolism: a single sample multi-omics approach. *Hormone and Metabolic Research* **53** 326–334. (<https://doi.org/10.1055/a-1440-0278>)
- Bechmann N & Eisenhofer G 2022 Hypoxia-inducible factor 2 α : a key player in tumorigenesis and Metastasis of pheochromocytoma and paraganglioma? *Experimental and Clinical Endocrinology and Diabetes* **130** 282–289. (<https://doi.org/10.1055/a-1526-5263>)
- Berends AMA, Eisenhofer G, Fishbein L, Van Der Horst-Schrivers ANAVD, Kema IP, Links TP, Lenders JWM & Kerstens MN 2019 Intricacies of the molecular machinery of catecholamine biosynthesis and secretion by chromaffin cells of the normal adrenal medulla and in pheochromocytoma and paraganglioma. *Cancers* **11** 1121. (<https://doi.org/10.3390/cancers11081121>)
- Bohn MC, Bloom E, Goldstein M & Black IB 1984 Glucocorticoid regulation of phenylethanolamine N-methyltransferase (PNMT) in organ culture of superior cervical ganglia. *Developmental Biology* **105** 130–136. ([https://doi.org/10.1016/0012-1606\(84\)90268-9](https://doi.org/10.1016/0012-1606(84)90268-9))
- Byrd JC, Hadjiconstantinou M & Cavalla D 1986 Epinephrine synthesis in the PC12 pheochromocytoma cell line. *European Journal of Pharmacology* **127** 139–142. ([https://doi.org/10.1016/0014-2999\(86\)90216-5](https://doi.org/10.1016/0014-2999(86)90216-5))
- Calsina B, Piñero-Yañez E, Martínez-Montes ÁM, Caleiras E, Fernández-Sanromán Á, Monteagudo M, Torres-Pérez R, Fustero-Torre C, Pulgarín-Alfaro M, Gil E, *et al.* 2023 Genomic and immune landscape of metastatic pheochromocytoma and paraganglioma. *Nature Communications* **14** 1122. (<https://doi.org/10.1038/s41467-023-36769-6>)
- Caratti B, Fidan M, Caratti G, Breitenecker K, Engler M, Kazemitash N, Traut R, Wittig R, Casanova E, Ahmadian MR, *et al.* 2022 The glucocorticoid receptor associates with RAS complexes to inhibit cell proliferation and tumor growth. *Science Signaling* **15** eabm4452. (<https://doi.org/10.1126/scisignal.abm4452>)
- Crona J, Delgado Verdugo A, Maharjan R, Ståhlberg P, Granberg D, Hellman P & Björklund P 2013 Somatic mutations in H-RAS in sporadic pheochromocytoma and paraganglioma identified by exome sequencing. *Journal of Clinical Endocrinology and Metabolism* **98** E1266–E1271. (<https://doi.org/10.1210/jc.2012-4257>)
- Crona J, Lamarca A, Ghosal S, Welin S, Skogseid B & Pacak K 2019 Genotype-phenotype correlations in pheochromocytoma and paraganglioma: a systematic review and individual patient meta-analysis. *Endocrine-Related Cancer* **26** 539–550. (<https://doi.org/10.1530/ERC-19-0024>)
- Currás-Freixes M, Piñero-Yañez E, Montero-Conde C, Apellániz-Ruiz M, Calsina B, Mancikova V, Remacha L, Richter S, Ercolino T, Rogowski-Lehmann N, *et al.* 2017 PheoSeq: a targeted next-generation sequencing assay for pheochromocytoma and paraganglioma diagnostics. *Journal of Molecular Diagnostics* **19** 575–588. (<https://doi.org/10.1016/j.jmoldx.2017.04.009>)
- Dunkley PR, Bobrovskaya L, Graham ME, Von Nagy-Felsobuki EI & Dickson PW 2004 Tyrosine hydroxylase phosphorylation: regulation and consequences. *Journal of Neurochemistry* **91** 1025–1043. (<https://doi.org/10.1111/j.1471-4159.2004.02797.x>)
- Eisenhofer G, Goldstein DS, Stull R, Keiser HR, Sunderland T, Murphy DL & Kopin IJ 1986 Simultaneous liquid-chromatographic determination of 3,4-dihydroxyphenylglycol, catecholamines, and 3,4-dihydroxyphenylalanine in plasma, and their responses to inhibition of monoamine oxidase. *Clinical Chemistry* **32** 2030–2033. (<https://doi.org/10.1093/clinchem/32.11.2030>)
- Eisenhofer G, Huynh TT, Pacak K, Brouwers FM, Walther MM, Linehan WM, Munson PJ, Mannelli M, Goldstein DS & Elkahloun AG 2004 Distinct gene expression profiles in norepinephrine- and epinephrine-producing hereditary and sporadic pheochromocytomas: activation of hypoxia-driven angiogenic pathways in von Hippel-Lindau syndrome. *Endocrine-Related Cancer* **11** 897–911. (<https://doi.org/10.1677/erc.1.00838>)
- Eisenhofer G, Lenders JW, Goldstein DS, Mannelli M, Csako G, Walther MM, Brouwers FM & Pacak K 2005 Pheochromocytoma catecholamine phenotypes and prediction of tumor size and location by use of plasma free metanephrines. *Clinical Chemistry* **51** 735–744. (<https://doi.org/10.1373/clinchem.2004.045484>)
- Eisenhofer G, Pacak K, Huynh TT, Qin N, Bratslavsky G, Linehan WM, Mannelli M, Friberg P, Grebe SK, Timmers HJ, *et al.* 2011 Catecholamine metabolomic and secretory phenotypes in pheochromocytoma. *Endocrine-Related Cancer* **18** 97–111. (<https://doi.org/10.1677/ERC-10-0211>)
- Eisenhofer G, Deutschbein T, Constantinescu G, Langton K, Pamporaki C, Calsina B, Monteagudo M, Peitzsch M, Flidner S & Timmers HJL 2020 Plasma metanephrines and prospective prediction of tumor location, size and mutation type in patients with pheochromocytoma and paraganglioma. *Clinical Chemistry and Laboratory Medicine* **1** 353–363. (<https://doi.org/10.1515/cclm-2020-0904>)
- Fang Z, Liu X & Peltz G. 2023 GSEApY: a comprehensive package for performing gene set enrichment analysis in Python. *Bioinformatics* **39** 757. (<https://doi.org/10.1093/bioinformatics/btac757>)
- Fishbein L, Leshchiner I, Walter V, Danilova L, Robertson AG, Johnson AR, Lichtenberg TM, Murray BA, Ghayee HK, Else T, *et al.* 2017 Comprehensive molecular characterization of pheochromocytoma and paraganglioma. *Cancer Cell* **31** 181–193. (<https://doi.org/10.1016/j.ccell.2017.01.001>)
- Grouzmann E, Tschopp O, Triponez F, Matter M, Bilz S, Brändle M, Drechsler T, Sigrist S, Zulewski H, Henzen C, *et al.* 2015 Catecholamine metabolism in paraganglioma and pheochromocytoma: similar tumors in different sites? *PLoS One* **10** e0125426. (<https://doi.org/10.1371/journal.pone.0125426>)
- Her S, Claycomb R, Tai TC & Wong DL 2003 Regulation of the rat phenylethanolamine N-methyltransferase gene by transcription factors Sp1 and MAZ. *Molecular Pharmacology* **64** 1180–1188. (<https://doi.org/10.1124/mol.64.5.1180>)
- Huynh TT, Pacak K, Wong DL, Linehan WM, Goldstein DS, Elkahloun AG, Munson PJ & Eisenhofer G 2006 Transcriptional regulation of phenylethanolamine N-methyltransferase in pheochromocytomas from patients with von Hippel-Lindau syndrome and multiple endocrine neoplasia type 2. *Annals of the New York Academy of Sciences* **1073** 241–252. (<https://doi.org/10.1196/annals.1353.026>)
- Jiang J, Zhang J, Pang Y, Bechmann N, Li M, Monteagudo M, Calsina B, Gimenez-Roqueplo AP, Nölting S, Beuschlein F, *et al.* 2020 Sino-European differences in the genetic landscape and clinical presentation of pheochromocytoma and paraganglioma. *Journal of Clinical Endocrinology and Metabolism* **105** 3295–3307. (<https://doi.org/10.1210/clinem/dgaa502>)

- Kanehisa M. 2002 The KEGG database. In *'In Silico' Simulation of Biological Processes: Novartis Foundation Symposium 247*. Chichester, UK: John Wiley & Sons. (<https://doi.org/10.1002/0470857897.ch8>)
- Lenders JWM, Kerstens MN, Amar L, Prejbisz A, Robledo M, Taieb D, Pacak K, Crona J, Zelinka T, Mannelli M, *et al.* 2020 Genetics, diagnosis, management and future directions of research of pheochromocytoma and paraganglioma: a position statement and consensus of the working group on endocrine hypertension of the European Society of Hypertension. *Journal of Hypertension* **38** 1443–1456. (<https://doi.org/10.1097/HJH.0000000000002438>)
- Li M, Prodanov T, Meuter L, Kerstens MN, Bechmann N, Prejbisz A, Remde H, Timmers HJLM, Nölting S, Talvacchio S, *et al.* 2023 Recurrent disease in patients with sporadic pheochromocytoma and paraganglioma. *Journal of Clinical Endocrinology and Metabolism* **108** 397–404. (<https://doi.org/10.1210/clinem/dgac563>)
- Lim JKM & Leprévier G 2019 The impact of oncogenic RAS on redox balance and implications for cancer development. *Cell Death and Disease* **10** 955. (<https://doi.org/10.1038/s41419-019-2192-y>)
- Love MI, Huber W & Anders S 2014 Moderated estimation of fold change and dispersion for RNA-seq data with DESeq2. *Genome Biology* **15** 550. (<https://doi.org/10.1186/s13059-014-0550-8>)
- Malumbres M & Barbacid M 2003 RAS oncogenes: the first 30 years. *Nature Reviews. Cancer* **3** 459–465. (<https://doi.org/10.1038/nrc1097>)
- Martins VR, Brentani MM & Housley PR 1995 Attenuation of glucocorticoid receptor levels by the H-ras oncogene. *Endocrine* **3** 305–312. (<https://doi.org/10.1007/BF03021410>)
- Mete O, Asa SL, Gill AJ, Kimura N, De Krijger RR & Tischler A 2022 Overview of the 2022 WHO classification of paragangliomas and pheochromocytomas. *Endocrine Pathology* **33** 90–114. (<https://doi.org/10.1007/s12022-022-09704-6>)
- Qin N, De Cubas AA, Garcia-Martin R, Richter S, Peitzsch M, Menschikowski M, Lenders JW, Timmers HJ, Mannelli M, Opocher G, *et al.* 2014 Opposing effects of HIF1 α and HIF2 α on chromaffin cell phenotypic features and tumor cell proliferation: insights from MYC-associated factor X. *International Journal of Cancer* **135** 2054–2064. (<https://doi.org/10.1002/ijc.28868>)
- Qin N, Peitzsch M, Menschikowski M, Siebert G, Pacak K & Eisenhofer G 2013 Double stable isotope ultra performance liquid chromatographic-tandem mass spectrometric quantification of tissue content and activity of phenylethanolamine N-methyltransferase, the crucial enzyme responsible for synthesis of epinephrine. *Analytical and Bioanalytical Chemistry* **405** 1713–1719. (<https://doi.org/10.1007/s00216-012-6599-x>)
- Sevilla LM, Jiménez-Panizo A, Alegre-Martí A, Estébanez-Perpiñá E, Caelles C & Pérez P 2021 Glucocorticoid resistance: interference between the glucocorticoid receptor and the MAPK signalling pathways. *International Journal of Molecular Sciences* **22** 10049. (<https://doi.org/10.3390/ijms221810049>)
- Stenman A, Welander J, Gustavsson I, Brunaud L, Bäckdahl M, Söderkvist P, Gimm O, Juhlin CC & Larsson C 2016 HRAS mutation prevalence and associated expression patterns in pheochromocytoma. *Genes, Chromosomes and Cancer* **55** 452–459. (<https://doi.org/10.1002/gcc.22347>)
- Vandevyver S, Dejager L & Libert C 2014 Comprehensive overview of the structure and regulation of the glucocorticoid receptor. *Endocrine Reviews* **35** 671–693. (<https://doi.org/10.1210/er.2014-1010>)
- Welander J, Łysiak M, Brauckhoff M, Brunaud L, Söderkvist P & Gimm O 2018 Activating FGFR1 mutations in sporadic pheochromocytomas. *World Journal of Surgery* **42** 482–489. (<https://doi.org/10.1007/s00268-017-4320-0>)
- Wurtman RJ & Axelrod J 1965 Adrenaline synthesis: control by the pituitary gland and adrenal glucocorticoids. *Science* **150** 1464–1465. (<https://doi.org/10.1126/science.150.3702.1464>)

Received 17 July 2023

Accepted 28 September 2023

Available online 29 September 2023

Version of Record published 30 October 2023